11.2

Induced nonlinear frequency shift of an active ring resonator on a magnonic crystal

© A.V. Bagautdinov, A.B. Ustinov

St. Petersburg State Electrotechnical University „LETI", St. Petersburg, Russia
E-mail: freester12@mail.ru

Received February 9, 2023
Revised April 7, 2023
Accepted May 4, 2023

The nonlinear shift of the resonant frequencies of a microwave active ring resonator (ARR) induced by a pump wave has been studied for the first time. The resonator was designed according to the scheme in the form of a closed ring containing a spin-wave delay line made on the basis of a one-dimensional magnonic crystal, as well as a microwave amplifier in a feedback circuit. It is shown, that with an increase in the power of the pumping wave, the shift of the resonant frequencies of the ARR increases in different ways depending on the position of the pumping frequency. The maximum induced nonlinear frequency shift is observed if the pumping frequency is at the minimum of the ARR transmission coefficient. A model describing the studied effect is developed.

Keywords: Magnonics, magnonic crystal, spin waves, magnetic films.

DOI: 10.61011/TPL.2023.07.56437.19527

Spin-wave active ring resonators (ARRs) have various fields of application. For example, they may be used to construct bistable devices [1], narrow-band microwave filters [2,3], matched filters [4], and microwave generators [5–11]. In recent years, artificial intelligence applications (specifically, magnonic reservoir computing [12–14]) have also become relevant.

It is known that electronic adjustment of characteristics of magnonic devices may be induced by different mechanisms. Magnetic reconstruction is currently one of the key mechanisms of this kind [15]. Electric adjustment with the use of ferrite–ferroelectric [3,16], ferrite–piezoelectric [17], and ferrite–semiconductor [18] structures is also possible.

The aim of the present study is to examine the nonlinear shift of resonance frequencies of a magnonic active ring resonator induced by a pump wave excited in it.

The schematic diagram of an active ring resonator is shown in Fig. 1, *a*. The setup includes a feedback circuit based on magnonic crystal *1*, microwave amplifier *2*, adjustable attenuator *3*, combiner *4*, and input *5* and output *6* directional couplers. The magnonic crystal in the feedback circuit was fabricated from an yttrium-iron garnet (YIG) film with thickness $L = 5.5\,\mu$m, saturation magnetization $M_0 = 153$ kA/m, and half-width $\Delta H = 48$ A/m of the ferromagnetic resonance curve. Twenty grooves with a depth of $0.5\,\mu$m were etched on the film surface. The prepared structure had period $\Lambda = 150\,\mu$m, wherein the width of etched (groove) and non-etched film parts was $a = 50\,\mu$m and $b = 100\,\mu$m, respectively. The YIG film was magnetized by a permanent magnet with field intensity $H = 97.6$ kA/m. A uniform bias field was applied in-plane along the grooves. Two short-circuited microstrip antennas with a width of $50\,\mu$m and a length of 2 mm were used to excite and receive surface spin waves in the YIG film. Distance d between the antennas was 7 mm. A microwave signal was fed to them along microstrip transmission lines with a wave impedance of 50 Ω. The microstrip circuit was fabricated by photolithography on a polycor substrate $500\,\mu$m in thickness. Amplifier *2* compensated the microwave signal loss in the delay line and other components of the ring. Adjustable attenuator *3* was used to control the signal amplification in the ring.

The concept of operation of the active ring resonator is as follows. A microwave signal is fed to input directional coupler *5* and starts circulating within the ring. After the completion of a single turn, the attenuated signal is combined with the input signal. Two signals then propagate within the ring. Following the completion of another turn, these signals are again combined with the input signal, raising the number of signals propagating within the ring to three. Thus, the microwave signal in the ring in steady-state operation is an infinite sum of decaying waves circulating within the ring. Resonance is established in the ring at certain frequencies satisfying the condition of in-phase summation of circulating waves. Total phase incursion $\Delta\varphi$ of the signal at these frequencies is a multiple of 2π [19].

The overall microwave signal amplification in the ring is characterized by effective gain G that is defined as the difference between amplifier gain *2* and microwave signal losses in other elements of the ring. If $G < 0$, the active ring resonator operates in the mode of microwave signal filtering. In the contrary case, the ring generates a microwave signal. It should be stressed that our earlier studies have been performed at $G < 0$ with the ring being essentially a ring resonator [2,3].

The induced nonlinear shift of resonance frequencies was examined by measuring the amplitude-frequency response (AFR) of the ARR. A signal from vector network analyzer *7*

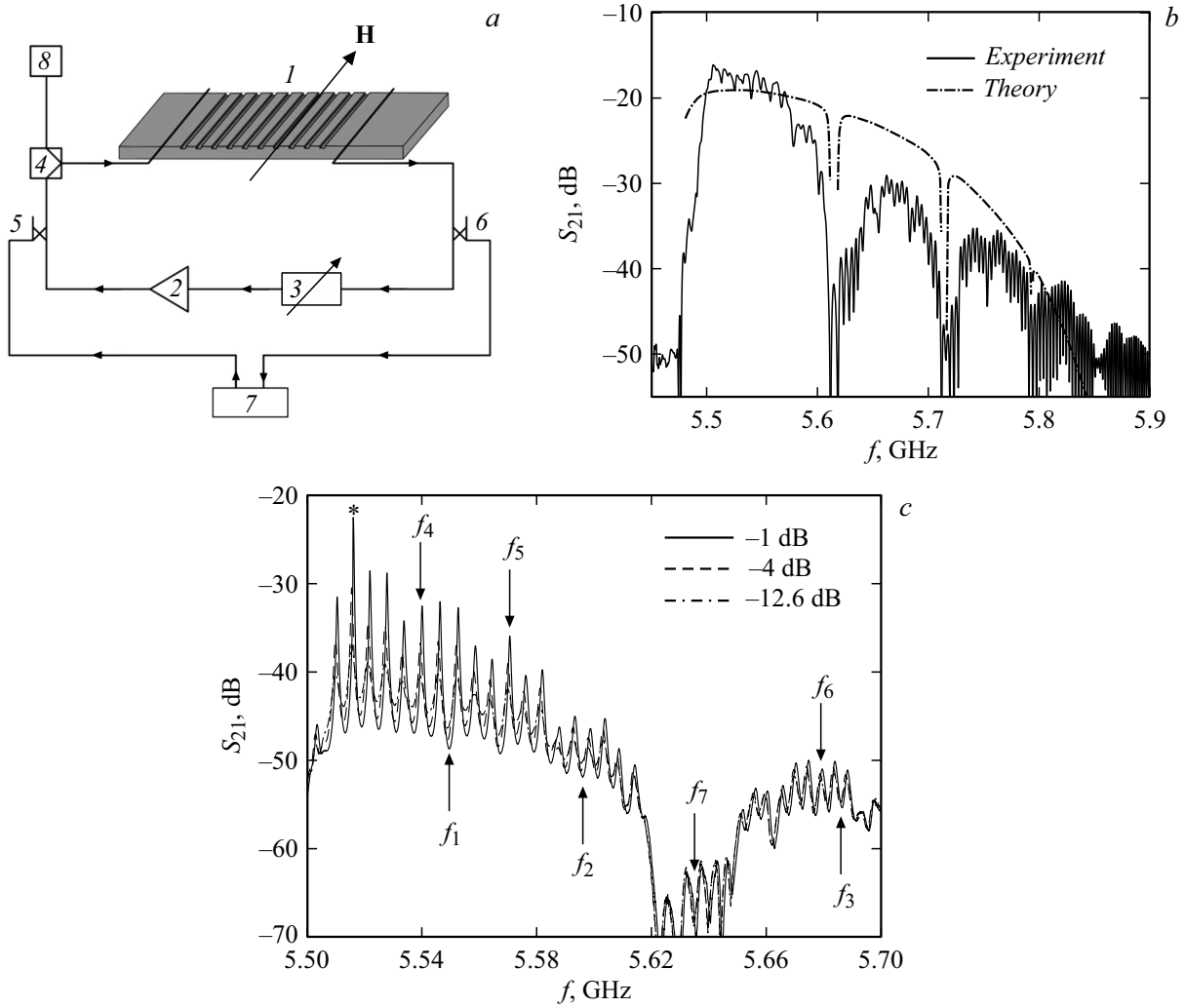

Figure 1. Schematic diagram of the experimental setup (a), amplitude-frequency response of the magnonic crystal (b), and resonance ARR curves for different values of effective gain G(c).

was introduced for this purpose into the ARR with the use of directional coupler *5*. The output ARR signal was extracted by directional coupler *6* and fed to the input terminal of the vector network analyzer. A microwave pump signal with a certain fixed frequency from generator *8* was fed to the magnonic crystal via combiner *4* for ARR frequency tuning. This signal induced a nonlinear phase shift [20] of the small-signal spin wave circulating in the ARR. This phase shift gave rise to a shift of resonance ARR frequencies. Just as in [20], the nonlinear mechanism establishing a nonlinear effect is the four-wave parametric interaction of spin waves.

Preliminary measurements of the magnonic crystal AFR (solid curve in Fig. 1, b) were performed first. The obtained AFR had characteristic dips at frequencies corresponding to bandgap frequencies of the magnonic crystal. The AFR calculated with both transmission and spin-wave excitation losses taken into account [21] is shown in the same figure (dash-and-dot curve). The ARR AFRs were measured after this; sections of the obtained curves are presented in Fig. 1, c. The peaks in these curves correspond to resonance frequencies of the ring. An asterisk denotes the resonance peak that was used to determine the nonlinear frequency shift induced by the pump signal introduced into the ring.

The principal measurements aimed at examining the induced nonlinear shift of resonance ARR frequencies were performed next. Pump signal frequencies lying between the resonance frequencies (f_1–f_3), at the resonance frequencies (f_4–f_6), and in the bandgap of the magnonic crystal (f_7) were chosen for the experiment (see Fig. 1, c). It was found that the resonance ARR frequencies decreased when the pump signal was applied. The typical plot illustrating the shift of the studied resonance peak is presented in Fig. 2, a. It can be seen that, in contrast to the case of bistability [22], the resonance curve underwent no nonlinear shape distortion. The resonance peak amplitude decreased with increasing pump signal power.

Symbols in Figs.2, b and c denote the results of experimental measurements of the nonlinear shift of the resonance peak frequency as function of the power level

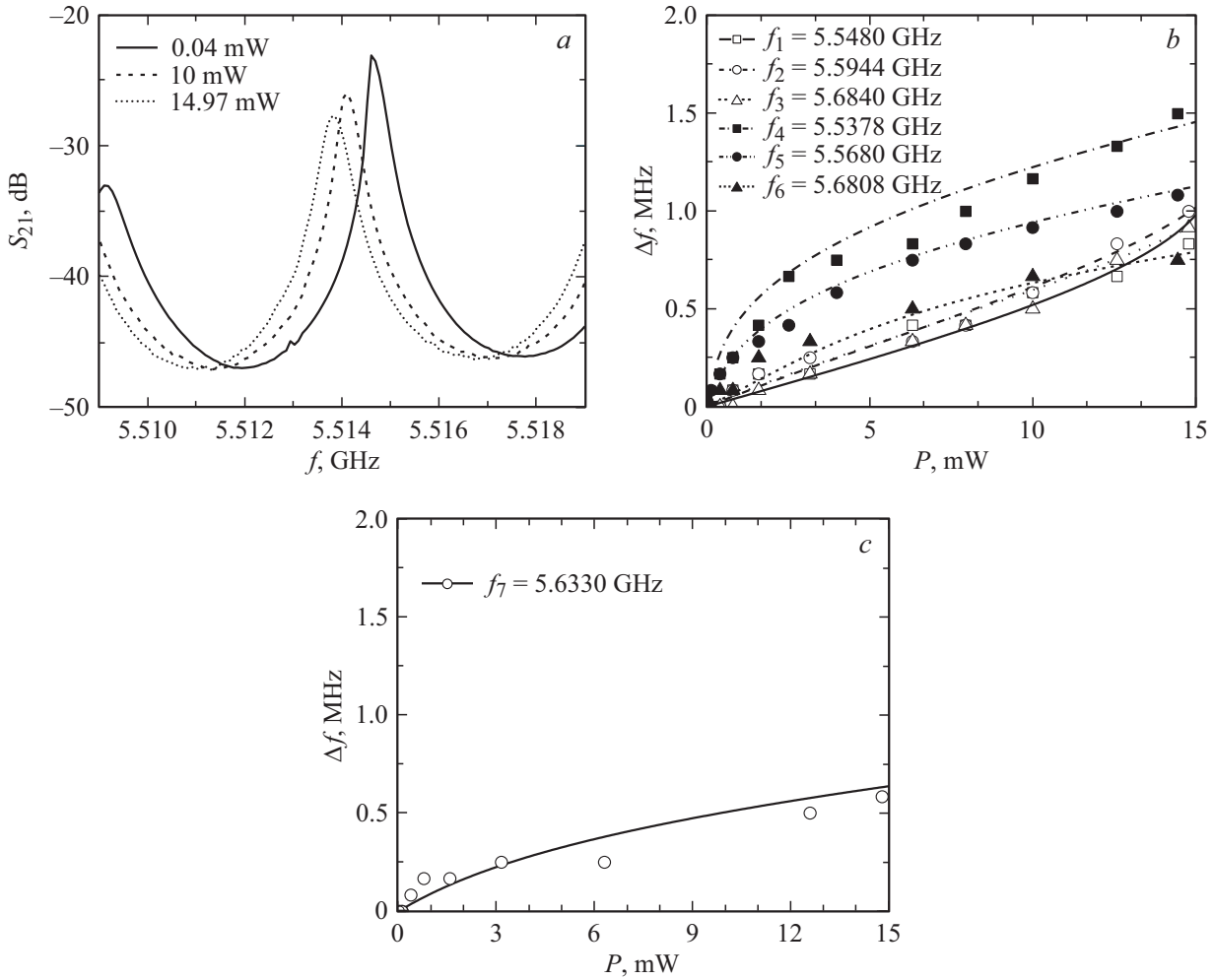

Figure 2. Resonance curves at different power levels of the pump signal with frequency f_1 (a). Experimental (symbols) and theoretical (curves) dependences of the induced nonlinear frequency shift on the pump signal power at minima f_1-f_3 and maxima f_4-f_6 (b) frequencies and at bandgap frequency f_7 of the magnonic crystal (c).

of the pump signal with various frequencies. The results of calculations performed using a theoretical model (see below) are represented by curves. It is evident that a pump wave excited at frequencies f_1-f_3 (i.e., between the resonance ARR peaks) induces a nonlinear frequency shift with a magnitude on the order of 1 MHz, which increases almost linearly with pump wave power up to 15 mW. This is attributable to the fact that the high-frequency ring resonance shifts toward the pump frequency as the pump power rises. In other words, the right resonance shifts down in frequency due to negativeness of the nonlinear coefficient of surface spin waves and gets closer to the pump frequency. At the same time, the low-frequency resonance shifts to the left (away from the pump frequency). When a pump signal with frequencies f_4-f_6, which correspond to ARR AFR maxima, is applied, the resonance peak is first shifted efficiently at low pump power values, but the shift at higher power levels is limited. This is due to the fact that the resonance ring frequency shifts away from the pump signal frequency as the pump power increases. Consequently, the growth of the pump wave power slows down, and the nonlinear frequency shift of the studied resonance ARR peak gets saturated along with it. If the pump signal frequency corresponds to the bandgap frequency (Fig. 2, c), the resonance frequency shift is weak. since spin waves decay rapidly in the bandgap of the magnonic crystal. In general, the presented plots demonstrate that the effect gets weaker at higher pump signal frequencies due to a reduction in the efficiency of excitation of spin waves.

A model characterizing the induced nonlinear shift of resonance ARR frequencies was developed in order to interpret the measured dependences. It follows from simple physical considerations that the resonance frequency shift is brought about by induced nonlinear phase shift $\Delta\varphi_{INL}$ of a spin wave travelling in the YIG film [20]. Therefore, the ARR power transmission factor is, in contrast to the linear model [19], written as

$$H_p(|u_p|^2) = \frac{0.5\exp(-\alpha d + g)}{\cosh(\alpha d - g) - \cos\left(kd + \Delta\varphi_{INL}(|u_p|^2)\right)}, \quad (1)$$

where $|u_p|$ is the normalized amplitude of precession of magnetization of a pump wave, α is the damping ratio, $g = \ln(10^{G/20})$ is the gain, and k is the wave number. The resonance nature of dependence $\Delta\varphi_{INL}$ $(|u_p|^2)$ was taken into account in the same way as in [22]. The resulting expression for $\Delta\varphi_{INL}$ had the following form:

$$\Delta\varphi_{INL}\left(|u_p|^2\right) = \frac{-0.5N_{12}|U_p|^2 dV_g^{-1}\exp(-\alpha d + g)}{\cosh(\alpha d - g) - \cos\left(kd + \Delta\varphi_{INL}(|u_p|^2)\right)}, \quad (2)$$

where N_{12} is the nonlinear coefficient for surface spin waves, $|U_p|^2$ is the squared absolute value of the dimensionless amplitude of an input microwave pump signal, and V_g is the group velocity. Expression (1) for H_p allows one to determine the normalized amplitude of a spin wave in the resonator: $|u_p|^2 = H_p|U_p|^2$. Curves in Figs. 2, *b* and *c* represent the results of calculation of the induced nonlinear frequency shift of the studied resonance ARR peak. It can be seen that the developed model provides a fine fit to experimental data.

It follows from the obtained results that a pump signal may be used to control the spectrum of resonance ARR frequencies. The maximum induced nonlinear frequency shift observed in our experiments (1.5 MHz) corresponds roughly to a quarter of the distance between resonance ARR frequencies. The examined effect has various potential applications. For example, it may be used to tune ARR frequencies and for data input into magnonic reservoir computers [12–14].

Funding

This study was supported financially by the Ministry of Science and Higher Education of the Russian Federation as part of a „Megagrant“ (agreement No. 075-15-2021-609).

Conflict of interest

The authors declare that they have no conflict of interest.

References

[1] Y.K. Fetisov, P. Kabos, C.E. Patton, Electron. Lett., **32** (20), 1894 (1996). DOI: 10.1049/el:19961254
[2] V.E. Demidov, B.A. Kalinikos, N.G. Kovshikov, P. Edenhofer, Electron. Lett., **35** (21), 1856 (1999). DOI: 10.1049/el:19991140
[3] A.B. Ustinov, G. Srinivasan, B.A. Kalinikos, Appl. Phys. Lett., **92** (19), 193512 (2008). DOI: 10.1063/1.2931085
[4] A.A. Porokhnyuk, A.B. Ustinov, N.G. Kovshikov, B.A. Kalinikos, Tech. Phys. Lett., **35** (9), 843 (2009). DOI: 10.1134/S106378500909017X.
[5] W. Ishak, Electron. Lett., **19** (22), 930 (1983). DOI: 10.1049/el:19830635
[6] S.N. Dunaev, Y.K. Fetisov, Electron. Lett., **28** (8), 789 (1992). DOI: 10.1049/el:19920498
[7] B.A. Kalinikos, M.M. Scott, C.E. Patton, Phys. Rev. Lett., **84** (20), 4697 (2000). DOI: 10.1103/PhysRevLett.84.4697
[8] A.D. Karenowska, A.V. Chumak, A.A. Serga, J.F. Gregg, B. Hillebrands, Appl. Phys. Lett., **96** (8), 082505 (2010). DOI: 10.1063/1.3318258
[9] A.B. Ustinov, A.A. Nikitin, B.A. Kalinikos, IEEE Magn. Lett., **6**, 3500704 (2015). DOI: 10.1109/LMAG.2015.2487238
[10] A.B. Ustinov, A.V. Kondrashov, A.A. Nikitin, V.V. Lebedev, A.N. Petrov, A.V. Shamrai, B.A. Kalinikos, J. Phys.: Conf. Ser., **1326** (1), 012015 (2019). DOI: 10.1088/1742-6596/1326/1/012015
[11] S.V. Grishin, O.I. Moskalenko, A.N. Pavlov, D.V. Romanenko, A.V. Sadovnikov, Y.P. Sharaevskii, I.V. Sysoev, T.M. Medvedeva, E.P. Seleznev, S.A. Nikitov, Phys. Rev. Appl., **16** (5), 054029 (2021). DOI: 10.1103/PhysRevApplied.16.054029
[12] S. Watt, M. Kostylev, Phys. Rev. Appl., **13** (3), 034057 (2020). DOI: 10.1103/PhysRevApplied.13.034057
[13] S. Watt, M. Kostylev, A.B. Ustinov, J. Appl. Phys., **129** (4), 044902 (2021). DOI: 10.1063/5.0033292
[14] S. Watt, M. Kostylev, A.B. Ustinov, B.A. Kalinikos, Phys. Rev. Appl., **15** (6), 064060 (2021). DOI: 10.1103/PhysRevApplied.15.064060
[15] V. Gevorkyan, V. Kochemasov, A. Ustinov, Kompon. Tekhnol., No. 4 (189), 25 (2017) (in Russian).
[16] A.B. Ustinov, A.V. Drozdovskii, A.A. Nikitin, A.A. Semenov, D.A. Bozhko, A.A. Serga, B. Hillebrands, E. Lähderanta, B.A. Kalinikos, Commun. Phys., **2**, 137 (2019). DOI: 10.1038/s42005-019-0240-7
[17] Y.K. Fetisov, G. Srinivasan, Appl. Phys. Lett., **88** (14), 143503 (2006). DOI: 10.1063/1.2191950
[18] M.A. Morozova, D.V. Romanenko, A.A.Serdobintsev, O.V. Matveev, Y.P. Sharaevskii, S.A. Nikitov, J. Magn. Magn. Mater., **514**, 167202 (2020). DOI: 10.1016/j.jmmm.2020.167202
[19] A.A. Nikitin, A.B. Ustinov, A.A. Semenov, B.A. Kalinikos, Tech. Phys., **57** (7), 994 (2012). DOI: 10.1134/S106378421207016X.
[20] A.B. Ustinov, N.A. Kuznetsov, R.V. Haponchyk, E. Lähderanta, T. Goto, M. Inoue, Appl. Phys. Lett., **119** (19), 192405 (2021). DOI: 10.1063/5.0074824
[21] B.A. Kalinikos, A.B. Ustinov, S.A. Baruzdin, *Spin-volnovye ustroistva i ekho-protsessy* (Radiotekhnika, M., 2013) (in Russian).
[22] V.V. Vitko, A.A. Nikitin, R.V. Haponchyk, A.A. Stashkevich, M.P. Kostylev, A.B. Ustinov, Eur. Phys. J. Plus, **137** (9), 1010 (2022). DOI: 10.1140/epjp/s13360-022-03213-5

Translated by D.Safin